The Application of Artificial Neural Network for Optimal Real-time Control of Microgrids

Luka Zoroje
School of Electrical Engineering
University of Belgrade
Belgrade, Serbia
0009-0005-9163-765X

Miodrag Forcan
University of East Sarajevo
School of Electrical Engineering
Sarajevo, BiH
0000-0002-1275-2870

Francisco de Paula García-López
Department of Electrical Engineering
University of Seville
Seville, Spain
0000-0003-3986-8483

Goran Dobrić
School of Electrical Engineering
University of Belgrade
Belgrade, Serbia
0000-0002-1747-6211

Jovana Forcan
University of East Sarajevo
Faculty of Philosophy,
Department of Computer Science
East Sarajevo, BiH
0000-0003-0354-3820

D. Marene Larruskain
School of Electrical Engineering
University of Basque Country EHU
Bilbao, Spain
0000-0003-3933-1504

Mileta Žarković
School of Electrical Engineering
University of Belgrade
Belgrade, Serbia
0000-0001-5855-6595

Manuel Barragán-Villarejo
Department of Electrical Engineering
University of Seville
Seville, Spain
0000-0003-0017-9162

Oihane Abarrategi
School of Electrical Engineering
University of Basque Country EHU
Bilbao, Spain
0000-0001-5360-2230

***Abstract*— Real-time optimisation of microgrids is essential to unlock the flexibility provided by distributed energy resources while keeping operating costs low. This paper proposes a lightweight Artificial Neural Network (ANN) controller that emulates an Optimal Power Flow (OPF) solver and delivers set-points to controllable generators, according to real-time conditions. A systematic workflow for (i) synthetic data generation, (ii) ANN architecture design and training, and (iii) the integration of trained ANN within hardware-in-the-loop (HIL) simulation setup using the OPAL-RT real-time platform is presented. Experiments on the benchmark CIGRE medium-voltage network demonstrate that the ANN achieves a low mean-squared error, enabling true real-time deployment. Compared with conventional OPF execution, the proposed ANN approach reduces CPU utilisation by more than 99 %, while preserving optimality within 0.52 %.**

***Keywords*— optimal power flow, neural networks, microgrids, real-time control**

I. Introduction

Microgrids are essential components of the Smart Grid vision, significantly improving reliability, resilience, and the integration of renewable energy sources. Their capability to operate both connected to the main grid and in islanded mode makes them highly suitable for applications such as rural electrification, campus energy management, and critical infrastructure support [1]. However, the inherent variability and uncertainty of solar and wind generation pose significant challenges to maintaining economic and secure microgrid operation. This necessitates frequent re-optimisation of power dispatch with fast and computationally efficient methods.

Traditional Optimal Power Flow (OPF) algorithms can find optimal dispatch solutions but are often computationally intensive and too slow for real-time or near-real-time control, especially on embedded hardware with limited processing capabilities. To address these limitations, recent research explores machine learning approaches, including deep reinforcement learning (DRL) [2], [3], and supervised deep neural networks (DNNs) [4]. For example, paper [2] develops a Double Dueling Deep Q Network (D3QN) to control energy storage systems in microgrids, optimizing power flow through reinforcement learning. Studies summarized in [3] systematically review DRL applications for microgrid control, highlighting their effectiveness for sequential decision-making under uncertainty. Meanwhile, [4] presents a DNN for day-ahead microgrid reconfiguration and dispatch, relying on forecasts of load and solar generation.

However, integrating these advanced learning methods into real-time embedded systems remains a key challenge due to the trade-off between accuracy, computational efficiency, and implementation feasibility. Addressing this gap, the present study contributes by developing a highly scalable synthetic dataset with 10,000 realistic OPF solutions, an ultra-lightweight artificial neural network (ANN), and rigorous hardware-in-the-loop (HIL) validation. Therefore, our contributions are threefold:

1. **High-fidelity synthetic dataset:** A scalable procedure to generate 10.000 OPF solutions that capture realistic correlations between load, renewable generation, and market prices.
2. **Ultra-light ANN:** A fully connected network that attains near-optimal dispatch accuracy while guaranteeing real-time computation on standard embedded CPUs.
3. **Hardware-in-the-loop (HIL) validation:** The integration and validation of trained ANN within hardware-in-the-loop (HIL) simulation setup using the OPAL-RT real-time platform.

The rest of the paper is organised as follows. Section II revisits the OPF formulation used to create datasets and introduces the benchmark system. Section III details the synthetic data generation workflow, describes the ANN architecture and training procedure and reports quantitative results. Section IV introduces simulation setup and discusses real-time HIL implementation. And finally, Section V concludes the paper with directions for future work.

II. Optimal Power Flow

A. Problem Statement

The AC OPF seeks to minimise the total operating cost of a microgrid (C_{tot}) while satisfying network power-flow

This is the author's accepted manuscript of a paper published in 2nd International Conference on Artificial Intelligence, Metaverse, and Cybersecurity (ICAMAC), Dubai, 2025
The final version of record is available via IEEE Xplore.

equations, voltage limits, and generator constraints. Mathematically:

$$\min_{P_G,Q_G,V,\theta} C_{tot} = \sum_{g\in\mathcal{G}} a_g\left(P_{G,g}\right)^2 + b_g\left(P_{G,g}\right) + c_g + p_{grid}P_{grid}$$

$$\text{s.t.} \quad \mathbf{f}(P_G, Q_G, V, \theta) = 0 \qquad \text{(AC PF)}$$

$$\underline{V} \le V_i \le \overline{V} \qquad \forall i \in \mathcal{N}$$

$$0 \le P_{G,g} \le \overline{P_{G,g}}, 0 \le Q_{G,g} \le \overline{Q_{G,g}}. \qquad \forall g \in \mathcal{G}$$

Here, a_g represents a quadratic coefficient of generation cost function ($/(kW)^2) of generator g, b_g is a linear coefficient of generation cost function ($/kW) of generator g, and c_g is a fixed start-up cost, which is omitted for real-time dispatch. The coefficient p_{grid} represents price of electrical energy that microgrid takes from the main grid. Parameters P_G, Q_G, V and θ represent active and reactive generation power, voltage magnitude and voltage angle of every node of the network, respectively. Letter $\mathcal{G}$ represents the set of controllable power sources from the network, which have constraint on the maximum active and reactive power, and $\mathcal{N}$ is set that contains every node of the network, which are limited by minimum and maximum voltage magnitudes. The first equation constraint is defined by the AC power flow equations in the network.

B. Case-Study Objective Function

CIGRE network (Figure 1), contains four controllable sources, including two residential fuel cells (FC-res), one combined heat and power (CHP) fuel cell (CHP-FC) and one CHP diesel aggregate (CHP-Diesel). If the active and reactive production power of renewable energy sources and the active and reactive power demand in every node of the microgrid is known, OPF can be easily performed. It is assumed that this grid represents a comprehensive MV microgrid. The objective function includes the total generation energy cost of four controllable assets, as well as the cost of energy delivered to the MV grid from the main grid. Table I summarises the adopted parameters.

TABLE I. GENERATION COST COEFFICIENTS OF CONTROLLABLE GENERATORS

Generator	*G1*	*G2*	*G3*	*G4*
Technology	FC-res	CHP-FC	CHP-Diesel	FC-res
Location (bus)	5	9	9	10
Nominal P (kW)	33	212	310	14
a_g ***($/(kW)^2)***	0.00481	0.00016	0.000272	0.00481
b_g ***($/kW)***	0.06885	0.06885	0.27839	0.06885
c_g ***($)***	0.74075	22.223	9.52408	0.74075

III. ANN CONTROLLER

A. Data Set Construction for ANN Training

The ANN controller developed in this study is supplied with exactly the same 32 measurements that the OPF solver requires. This full-observability configuration guarantees a *like-for-like* benchmark on the OPAL-RT real-time platform: any performance difference between OPF and ANN can be attributed solely to the computational method. Once parity is demonstrated, we will investigate low-impact features and retrain the network, opening operating regimes in which classical OPF cannot converge because the necessary measurements are unavailable or too costly to obtain. Table II explains all input data.

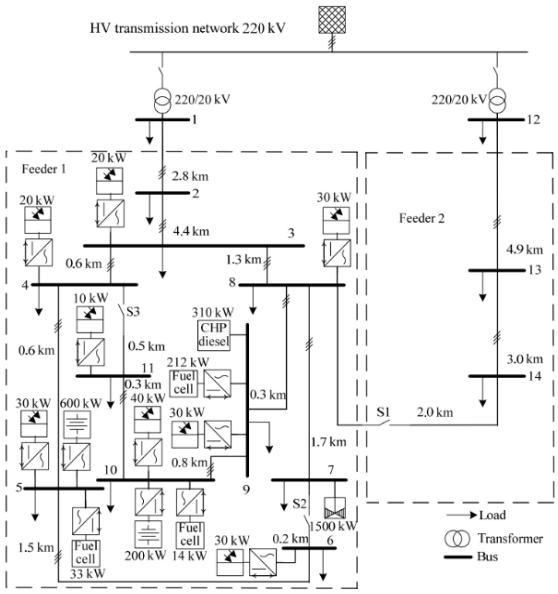

Fig. 1. Medium voltage CIGRE network [5]

TABLE II. SIGNAL INVENTORY

Category	***Signals***	***Rationale***
System demand	26	Active (P) and reactive (Q) power at each of the 13 *electrically distinct* buses. Buses 1 and 12 are galvanically identical; their demands are aggregated, reducing the count from 14 to 13 buses.
Renewables	2	(i) Aggregate PV output—eight rooftop arrays share a proportional profile due to uniform insolation, so a single per-unit measurement suffices; (ii) output of a single wind farm.
Market prices	3	Real-time diesel, fuel-gas, and grid-import tariffs used in the OPF cost function.
Network state	1	Slack-bus voltage magnitude (V1V_1V1), allowed to drift ±5 % around nominal.

A database of 9600 operating points (400 days × 24 h) was created, by varying:

1. **Load time-series:** Typical load profiles from [5] were used, and varied ±20% to emulate different operating points
2. **PV time-series:** Derived from European reference curves and scaled by a uniform random factor to emulate seasonal and daily variability.
3. **Wind time-series:** Having a random value up to nominal wind power.
4. **Price:** Each tariff is perturbed ±20% around its historical mean, teaching the ANN to cope with market volatility.
5. **Slack-bus voltage:** Randomly varied within ±5 % of nominal to reflect on-load tap-changer action.

The resulting dataset pairs a 32-dimensional input vector with a 4-dimensional output vector (Figure 2).

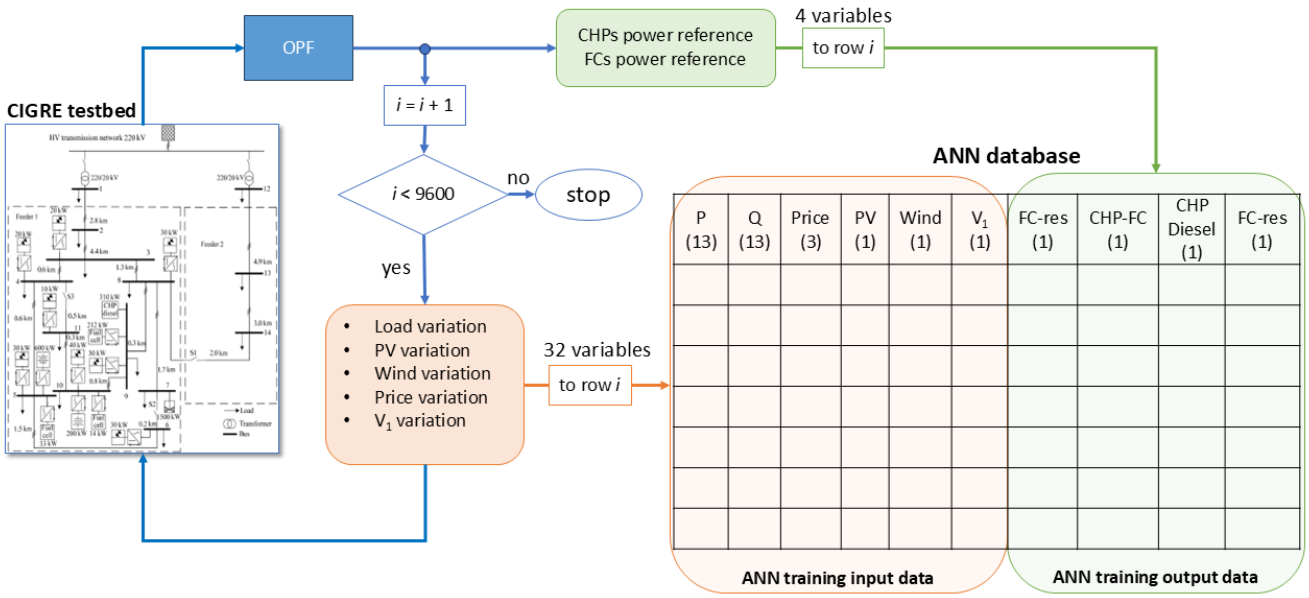

Fig. 2. Data Set Construction for ANN Training

In the future-work, feature-importance analysis will identify redundant measurements; the ANN will then be retrained with partial input vectors. Such reduced-telemetry scenarios are intractable for classical OPF, but remain solvable with data-driven approach.

B. Artificial-Neural-Network Design and Training

Embedding the full AC-OPF for a real-time control is computationally prohibitive on most field controllers. A forward pass through a trained ANN, by contrast, delivers set-points in real time, making it ideal for hardware-in-the-loop (HIL) studies.

A compact multilayer perceptron was selected after hyper-parameter sweeps (Figure 3). The most popular sort of ANN is made up of three sets of layers: input layer, hidden layers and output layers [6] and it can easily model complex or multi complex tasks [7].

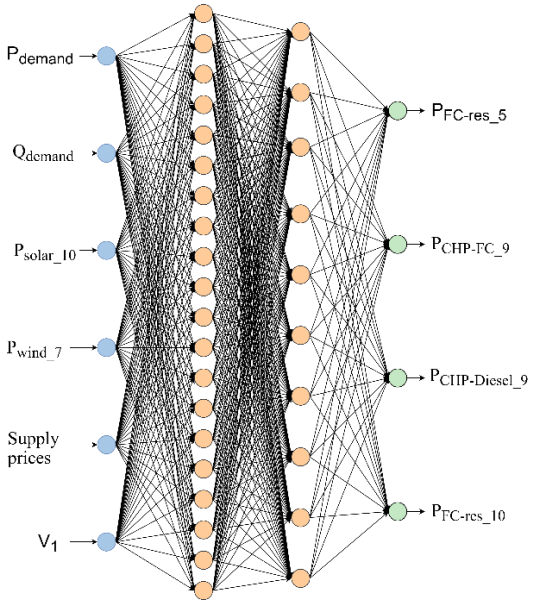

Fig. 3. ANN selected for AC OPF problem of the CIGRE network

The trained network is exported via *gensim* as an S-function for OPAL-RT. It was adopted for ANN model from this paper to have two hidden layers, the first layer with twenty nodes and the second with ten nodes. All nodes in hidden layers have the hyperbolic tangent sigmoid activation function, while nodes from output layers have linear activation function.

After training ANN, values of production power of controllable energy sources from the microgrid in comparison with values obtained from the OPF code are shown in four graphics in Figure 4. Generator 1, in the first graphic, corresponds to the fuel cell with nominal power of 33 kW located in bus 5. Generator 2, in the second graphic, corresponds to the CHP fuel cell with nominal power of 212 kW located in bus 9. Generator 3, in the third graphic, corresponds to the CHP diesel aggregate with nominal power of 310 kW located also in bus 9. Finally, generator 4 corresponds to the fuel cell with nominal power of 14 kW located in bus 10.

The accuracy of the artificial neural network (ANN) is evaluated using several error metrics: MAPE (Mean Absolute Percentage Error), MAE (Mean Absolute Error), MSE (Mean Squared Error), and RMSE (Root Mean Squared Error). MAE reflects the average magnitude of the differences between the actual and predicted values. MSE assesses the average of the squared differences between these values, emphasizing larger errors. RMSE, as the square root of MSE, provides an interpretable measure of the average prediction error in the same units as the target variable. By calculating multiple error metrics, a more comprehensive and reliable assessment of the model's performance and deviation from true values is achieved.

TABLE III. CALCULATED ERRORS FOR ANN

$MAPE = \frac{\sum_{i=1}^{N} \frac{\lvert y - y_i \rvert}{y}}{N} \cdot 100\ \% = 0.52\ \%$ (with 99.2 % of data)
$MAE = \frac{\sum_{i=1}^{N} \lvert y_i - y \rvert}{N} = 0.1018\ \text{kW}$
$MSE = \frac{\sum_{i=1}^{N} (y - y_i)^2}{N} = 0.0686\ (\text{kW})^2$
$RMSE = \sqrt{\frac{\sum_{i=1}^{N} (y - y_i)^2}{N}} = 0.2619\ \text{kW}$

In Table III, N is dimension of data set and y_i is the predicted value and y is real value. The error coefficient MAPE is calculated by using 99.2 % of predicted and real values from data set. Other 0.8 % values from data set are very close to zero, so they make large percentage errors in MAPE calculation, but not large absolute errors. Those values are not relevant ANN performance indicators, so they are excluded from MAPE calculation.

IV. IMPLEMENTING THE ANN IN SIMULATION

Once the ANN is successfully trained and its performance validated, it can be seamlessly integrated into the SIMULINK environment using the MATLAB command *gensim(net, st)*, where *net* represents the trained neural network and *st* is the simulation sampling time—set to 50 µs in this case (the time of OpalRT timestep).

To simulate the ANN-based control in real time, the OPAL-RT simulator introduced earlier is used. The overall simulation is divided into two subsystems: a master block, which contains the microgrid model and power system dynamics, and a slave block, which includes control logic such as the ANN function block. Figure 5 illustrates the structure of the master block and Figure 6 illustrates the structure of the slave block.

As can be seen in graphics shown in Figure 4, ANN trained as described in the previous section, with set of input signals also described before, makes very accurate prediction of optimal production power of controllable energy sources that exist in the microgrid. Calculated mean squared error value of ANN prediction is 0.0686 $(\text{kW})^2$, which is also an indicator of a very accurate prediction.

While the present ANN uses the full OPF feature set for a rigorous baseline, its true advantage emerges when inputs are scarce, delayed, or noisy—conditions under which classical OPF becomes inoperable. Ongoing research will:

1. Rank feature importance and prune low-impact signals.
2. Retrain and validate reduced-input ANNs on HIL platforms.
3. Deploy the smallest viable network on low-cost ARM microcontrollers, extending optimal dispatch capabilities to resource-constrained microgrids.

Communication between the master and slave blocks is managed using the OPComm block, which facilitates data exchange at each simulation time step. The Memory block ensures that data from previous steps is retained and made available for consistent synchronization. This setup guarantees that both the power system (master) and the control logic (slave) execute concurrently and deterministically, without timing overruns. By compiling the slave block with the ANN into OPAL-RT's real-time environment, the ANN can respond to changes in the microgrid in real time, enabling reliable hardware-in-the-loop (HIL) validation under real-time conditions.

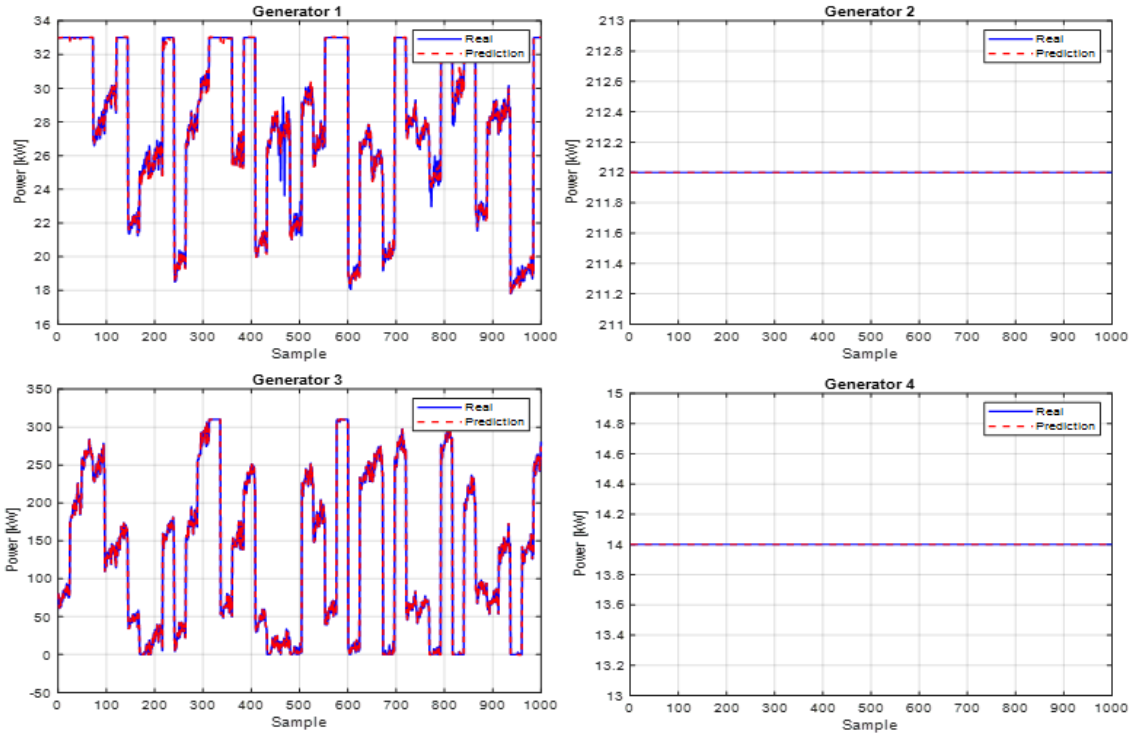

Fig. 4. ANN performance compared to real values from OPF – results for all controllable sources in the microgrid

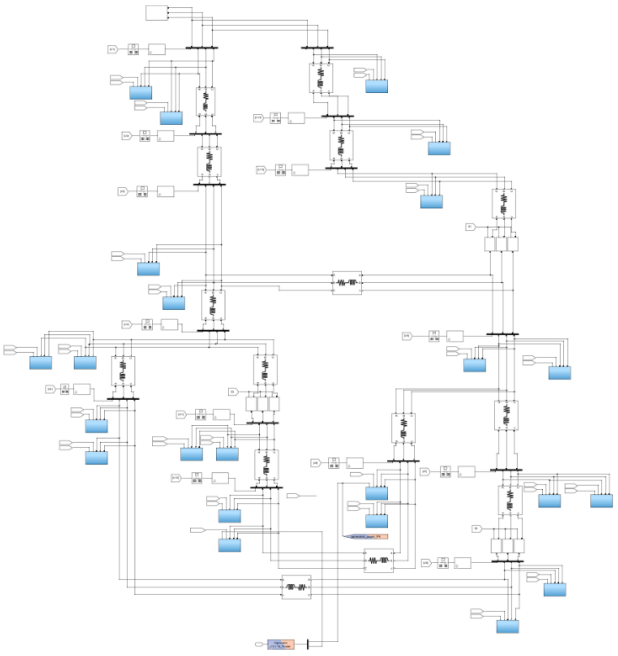

Fig. 5. The microgrid model made in RT-Lab

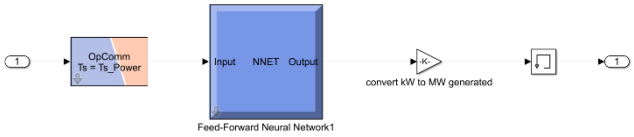

Fig. 6. ANN function block made in RT-Lab

V. Testing The ANN With Limited Input Data

In this section, an analysis was conducted to evaluate the performance of the ANN implemented in this paper, that was trained with all input data as OPF, if one input data is missing. The test was conducted by setting one input variable to zero for every hour of the year, and the procedure was done for active and reactive power demand of every node of the network and power production from renewable energy sources. The value of Mean Squared Error (MSE) for every input variable missing is shown in table IV. Results for active and reactive power demand in node 2 of the network are not shown in the table IV because those variables were already zero - node 2 is a transit mode and there is no power demand in it.

The analysis shows that the model produces a noticeable Mean Squared Error (MSE), compared to 0.0686 $(kW)^2$ with no input variable missing, for every input feature tested. This indicates that the predictions of ANN, trained as previously described, are consistently affected by changes in each input variable. In other words, no single input is irrelevant to the model: every input contributes in some way to the output, and small perturbations lead to measurable deviations. The ANN performance for the case when the data of active power demand in node 5 is missing, where the value of MSE is the biggest out of every node, is shown in figure 7. Only predictions of Generator 1 and 3 are shown because all the predictions for Generator 2 and 4 are the same as in Figure 4.

TABLE IV. Testing ANN when one input data is missing

Missing data	MSE $[(kW)^2]$	Missing data	MSE $[(kW)^2]$
Pd1	78.8319	**Qd3**	8.1382
Pd3	1.1999	**Qd4**	13.1330
Pd4	25.6174	**Qd5**	97.5537
Pd5	103.2103	**Qd6**	91.9467
Pd6	60.5134	**Qd7**	4.2820
Pd7	5.4088	**Qd8**	9.8962
Pd8	7.2244	**Qd9**	71.2693
Pd9	28.3541	**Qd10**	82.7741
Pd10	34.2405	**Qd11**	3.9770
Pd11	14.7808	**Qd12**	24.2161
Pd12	38.3797	**Qd13**	16.0861
Pd13	10.1451	**Psolar**	0.1367
Qd1	16.2460	**Pwind**	24.0011

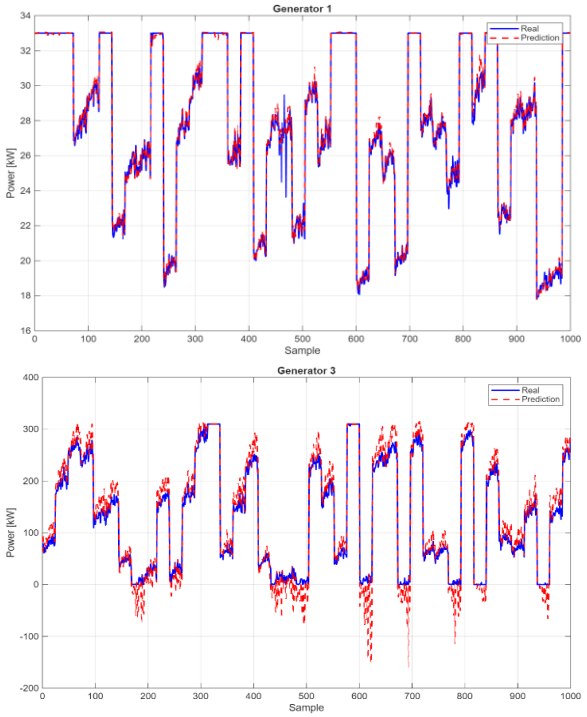

Fig. 7. ANN performance when Pd_5 is missing

When it comes to the market price of diesel and fuel gas, the ANN also shows high sensitivity. Apart from that, this analysis proves the accuracy of the OPF code used in ANN training process, because in case that diesel price is equal to zero, ANN sends signal to CHP-Diesel aggregate to produce energy with almost nominal power and vice versa. Those results are shown in figure 8 and 9 for diesel and fuel price missing, respectively.

Along with the performed measurements, the determination of the partial correlation coefficient between each input and output variable was also conducted. The measurements show that the highest absolute value of partial correlation coefficient occurs between diesel price and power production of CHP diesel aggregate, and its value is -0.977, which is expected given the previously presented figures.

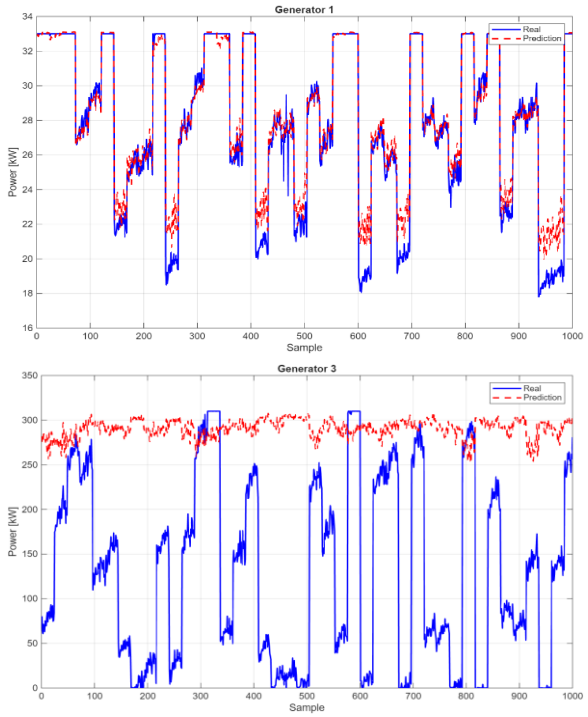

Fig. 8. ANN performance when diesel price is missing

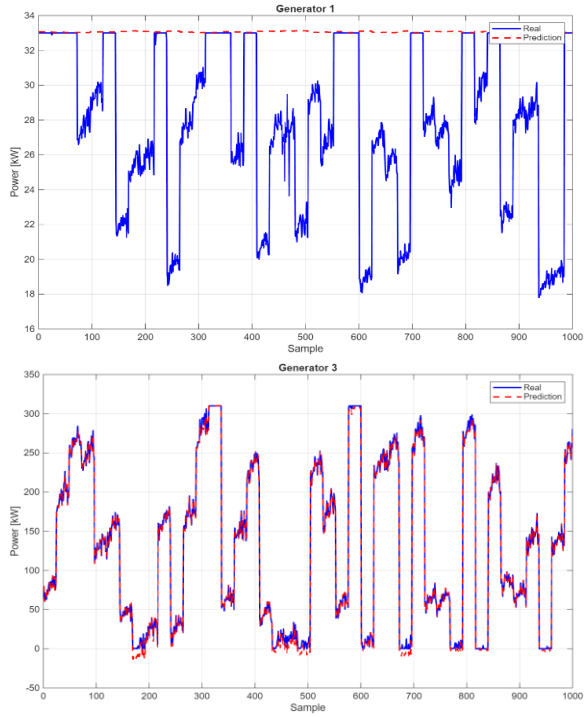

Fig. 9. ANN performance when fuel gas price is missing

VI. Conclusion

This paper presented an ANN approach for optimal power flow (OPF) control in microgrids, designed to operate in real time on hardware-in-the-loop (HIL) simulators. By using the same 32 input signals as the classical OPF solver, the ANN enables a fair, one-to-one comparison and demonstrates its ability to deliver near-optimal dispatch decisions with a mean squared error of 0.069 kW² and a cost deviation of just 0.52 %. Real-time implementation on an OPAL-RT platform confirmed that the ANN achieves sub-millisecond inference times—reducing CPU load by more than 99 % compared to iterative OPF—while preserving dispatch accuracy. This analysis was conducted on Intel Core Ultra 7 Processor 155HL, that has performance-core base frequency of 1.4 GHz.

Although this study focuses on full-input configurations to validate ANN performance under ideal observability, the real benefit of the approach lies in its ability to function reliably even when some measurements are missing, delayed, or expensive to acquire. Therefore, this paper also presented the sensitivity of ANN to missing input data, as an introduction to future work that will explore reduced-input configurations, dynamic retraining, and deployment on embedded hardware to bring OPF-grade intelligence to low-cost microgrid controllers. These steps will enable real-time optimization in settings where classical OPF is infeasible, paving the way for scalable, flexible, and efficient control in next-generation distribution networks.

VII. Acknowledgment

This publication is part of the project SUNRISE and it has been supported by the European Commission under grant agreement 101079200.

The research was partially conducted in the premises of the Palace of Science, Miodrag Kostić Endowment.

References

[1] D. T. Ton and M. A. Smith “The U.S. department of energy’s microgrid initiative”, The Electricity Journal, Volume 25, Issue 8, October 2012, Pages 84-94

[2] F. Yao, W. Zhao, M. Forshaw and Y. Song “A holistic power optimization approach for microgrid control based on deep reinforcement learning”, January 2024, DOI: 10.2139/ssrn.4836395, unpublished

[3] N. F. P. Dinata, M. A. M. Ramli, M. I. Jambak, M. A. B. Sidik and M. M. Alqahtani “Desining and optimal microgrid control system using deep reinforcement learning: A systematic review”, Engineering Science and Technology, an International Journal, Volume 51, March 2024, 101651

[4] F. Yaprakdal, M. B. Yilmaz, M. Baysal, A. Anvari-Moghaddam “A deep neural network-assisted approach to enhance short-term optimal operational sheduling of a microgrid”, Sustainability, February 2020

[5] Rudion, K., Orths, A., Styczynski, Z. A., & Strunz, K. (2006, June). Design of benchmark of medium voltage distribution network for investigation of DG integration. In *2006 IEEE power engineering society general meeting* (pp. 6-pp). IEEE.

[6] R. Qamar, B. A. Zardari “Artificial neural networks: An overview”, Mesopotamian journal of Computer Science, 2023, pp. 130-139, DOI: https://doi.org/10.58496/MJCSC/2023/015

[7] L. Lazli, M. Boukadoum “Hidden neural network for complex pattern recognition: a comparison study with Multi-nrural network-based approach”, International Journal od Life Science and Medical Research, 2013, 234-24